ISBN: 978-3-95450-179-3 doi:10.18429/JACoW-FEL2017-WEP060

CHARACTERIZING SUB-FEMTOSECOND X-RAY PULSES FROM THE LINAC COHERENT LIGHT SOURCE

S. Li*, R. Coffee, K. Hegazy, Z. Huang, A. Natan[1], T. Osipov, D. Ray, J. Cryan[1], and A. Marinelli,
SLAC National Laboratory, Menlo Park, United States
[1]also at Stanford PULSE Institute, Menlo Park, United States
Z. Guo, Stanford University, Stanford, United States

Abstract

The development of sub-femtosecond x-ray capabilities at the Linac Coherent Light Source requires the implementation of time-domain diagnostics with attosecond (as) time resolution. Photoelectrons created by attosecond duration x-ray pulses in the presence of a strong-laser field are known to suffer an energy spread which depends on the relative phase of the strong-laser field at the time of ionization. This phenomenon can be exploited to measure the duration of these ultrashort x-ray pulses. We present an implementation which employs a circularly polarized infrared laser pulse and novel velocity map imaging design which maps the phase dependent momentum of the photoelectron onto a 2-D detector. In this paper, we present the novel co-linear VMI design, simulation of the photoelectron momentum distribution, and the reconstruction algorithm.

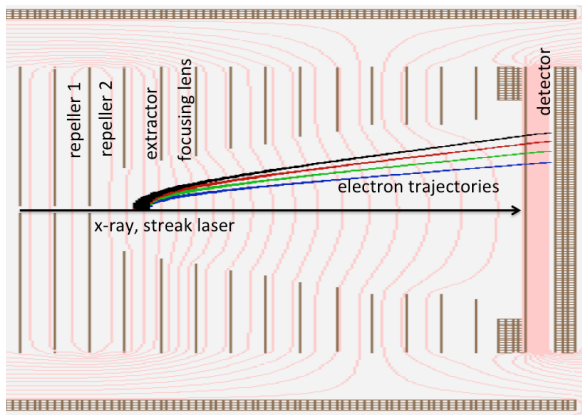

Figure 1: Side view of the cVMI design, with the linearly polarized x-ray pulse and circularly polarized streaking laser pulse propagating co-linearly. Picture taken in SIMION-8.0.

INTRODUCTION

Electron motion in atoms and molecules is the essential key to understanding the earliest processes involved in chemical changes. Electrons move across a molecular bond in 0.1 to 1 femtosecond (fs), a time scale of which direct measurement was impossible until recently when high harmonic generation [1, 2] became a widely used tool to synthesize light pulse in the extreme ultra-violet regime with sub-femtosecond duration. Extending the photon wavelength to the soft x-ray regime, the enhanced self-amplified spontaneous emission (eSASE) from x-ray free electron lasers enables the production of high intensity attosecond pulses [3]. The method of eSASE is currently being implemented experimentally at the linac coherent light source (LCLS) [4]. The electron bunch goes through an emittance spoiler which destroys the bunch except for a femtosecond duration beam core. The unspoiled core then interacts with an optical laser which imprints energy modulation on to the beam. Going through a dispersive section, the energy modulation turns into a single current spike with sub-femtosecond duration. The current spike goes through the undulator which emits coherent attosecond x-ray pulses.

Therefore, in order to measure the temporal profiles of sub-femtosecond x-ray pulses we employ a variant of the well known "attosecond streak camera" technique [5]. Our variation, which is closely related to the "atto-clock" technique [6], exploits the correlation between optical-cycle phase and streaking direction in a circularly polarized laser pulse. The photoelectrons generated by the attosecond x-ray pulse interacting with gas molecules in the presence of a strong laser field experience an energy spread which depends on the duration of these ultrashort x-ray pulses. With a circularly polarized streaking laser, we provide a kick to the photoelectrons momentum distribution, and the angle and the strength of the momentum shift contains timing information of the x-ray pulse. Similar work has been done with longer x-ray pulses and a detector that measures a slice of the photoelectron momentum distribution [7]. With our novel co-linear velocity map imaging (cVMI), we will measure a 2-D projection of the 3-D momentum distribution of electrons generated by the linearly polarized attosecond x-ray pulse and the circularly polarized IR streaking pulse.

We develop an algorithm to reconstruct the x-ray pulse from the 2-D photoelectron momentum distribution. We use the von Neumann representation [8] to decompose the x-ray pulse into a set of basis functions. The fitting algorithm searches for the complex coefficients related to the basis functions by minimizing the difference between the measurement image and the fitted image. We demonstrate that we can successfully reconstruct attosecond x-ray pulses generated from free electron laser simulations.

VMI DESIGN

A VMI spectrometer has the advantages of high collection efficiency and high angular resolution. The critical requirement for a VMI to work is to image the charged particles with the same momentum onto the same position on the

* siqili@slac.stanford.edu

Content from this work may be used under the terms of the CC BY 3.0 licence (© 2018). Any distribution of this work must maintain attribution to the author(s), title of the work, publisher, and DOI.

ISBN: 978-3-95450-179-3 doi:10.18429/JACoW-FEL2017-WEP060

Content from this work may be used under the terms of the CC BY 3.0 licence (© 2018). Any distribution of this work must maintain attribution to the author(s), title of the work, publisher, and DOI.

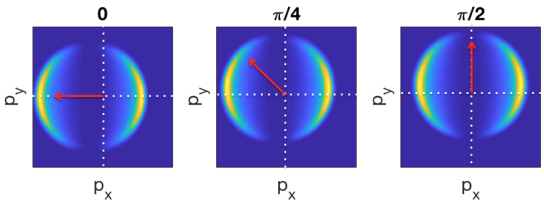

Figure 2: Simulation of the measured VMI image with a FWHM 300as x-ray pulse streaked by a 1.3μm laser. From left to right we vary the relative phase between the x-ray pulse and the streaking laser pulse to be 0, $\pi/4$, and $\pi/2$ respectively. The red arrows illustrate the direction of the momentum kick relative to the center of the image.

two-dimensional detector, regardless of the particles' initial position. This is achieved by arranging the metal plates with specific voltages in the spectrometer to create electro-static field that images the photoelectrons. Our co-linear VMI design follows a similar procedure as described in [9]. Instead of a traditional VMI configuration [10], we include a focusing lens plate and several subsequent plates for enhancing energy resolution to treat the novel setup where the x-ray and streaking laser propagate co-linearly. We use an ion-tracking program, SIMION-8.0, to simulate electron motions in the VMI. Figure 1 is a side view of the cylindrically-symmetric spectrometer.

The energy resolution of the VMI is determined by simulating trajectories of groups of charged particles with different central energy, 0.3 standard deviation in energy, and a uniformly-distributed initial momentum direction. Our cVMI design is capable of distinguishing 3% energy difference among the particle groups. For the purpose of diagnosing photoelectrons generated by attosecond pulses which necessarily have a large bandwidth, above 3eV, our VMI design provides sufficient energy resolution.

STREAKING SIMULATION

We base our simulation of the streaking process on the Lewenstein model [11]. Under the strong field approximation, the governing equation to calculate the transition amplitude as a function of photoelectron's final momentum, $b(\vec{p})$, of the continuum states of atoms in the presence of strong laser field is expressed as follows,

$$b(\vec{p}) = -i \int_{-\infty}^{+\infty} dt \vec{E}(t) \cdot \vec{d}(\vec{p} + \vec{A}(t)) \exp\{i\Phi(t)\}, \quad (1)$$

and

$$\Phi(t) = -\int_{t}^{+\infty} dt' [(\vec{p} + \vec{A}(t'))^2/2 + I_p]. \quad (2)$$

In Eq. 1 and 2, $\vec{E}$ is the total electric field, $\vec{d}$ is the dipole moment for the transition to the continuum states, $\vec{A}$ is the vector potential of the streaking laser, and I_p is the ionization potential of the atom. The integral in the exponential starts from the time of ionization, t, to ∞, and the outer integral expands entire time to allow any time of ionization. Because the x-ray pulse contains much higher frequency components compared to the streaking laser pulse, only the x-ray field contributes to the outer integral to compensate for the fast oscillating phase Φ. We can replace the total electric field $\vec{E}$ with the x-ray electric field $\vec{E_X}$. Note that Eq. 1 calculates the transition amplitude as a function of a photoelectron's final 3-D momentum, $b(p_x, p_y, p_z)$. However, what we measure with a VMI spectrometer is the probability distribution of a photoelectron's 2-D momentum,

$$B(p_x, p_y) = \int dp_z \left| b(p_x, p_y, p_z) b^*(p_x, p_y, p_z) \right|. \quad (3)$$

An important feature of angular streaking is that the circularly polarized streaking laser imposes a momentum kick to the photoelectrons as a function of time. The strength and the angle of the kick is determined by the relative phase between the x-ray pulse and the streaking laser pulse. In Fig. 2 we demonstrate the simulated photoelectron momentum distribution projected onto a 2-D VMI detector, while varying the relative phase between the x-ray pulse and the streaking laser pulse. The apparent double-arc shape comes from the dipole moment $\vec{d}$ in Eq. 1.

RECONSTRUCTION ALGORITHM

Traditionally VMI images are analyzed with inverse Abel transform due to cylindrical symmetry [12]. This is not possible for our VMI design because angular streaking breaks the cylindrical symmetry. However, since we know the physics of the streaking process, we can limit the reconstruction to a small subset of all possible momentum distributions.

The basic idea of our reconstruction algorithm is to decompose the measured VMI image into "basis images" and the complex coefficients corresponding to each basis give the reconstructed x-ray pulse. As shown in Eq. 1, the transition amplitude is linearly proportional to the x-ray electric field, $b(\vec{p}) \propto \vec{E_X}(t)$. If we decompose $\vec{E_X}(t)$ into a sum of basis functions, then we can write $b(\vec{p}) = \sum_n c_n b_n(\vec{p})$, where we allow the coefficients c_n to be complex. The measured 2-D momentum distribution becomes

$$\begin{aligned} B(p_x, p_y) &= \sum_n \sum_m \int dp_z c_n^* c_m b_n^*(\vec{p}) b_m(\vec{p}) \\ &= \sum_n \sum_m c_n^* c_m B_{nm}(p_x, p_y), \end{aligned} \quad (4)$$

where $\vec{p}$ denotes the 3-D momentum, and $B_{nm}(p_x, p_y)$ is what we refer to as the "basis image".

To decompose the electric field, we choose the von Neumann representation to describe the x-ray electric field [8], which includes the intensity and phase information of the x-ray pulse in both the time and the frequency domain. The von Neumann basis function is

$$\alpha_{\omega_i t_j}(t) = \left(\frac{1}{2\alpha\pi}\right)^{\frac{1}{4}} \exp\left[-\frac{1}{4\alpha}(t - t_j)^2 - it\omega_i \right], \quad (5)$$

where t_i and ω_j are the time and frequency axis in the von Neumann representation, α is a constant determined by the

ISBN: 978-3-95450-179-3 doi:10.18429/JACoW-FEL2017-WEP060

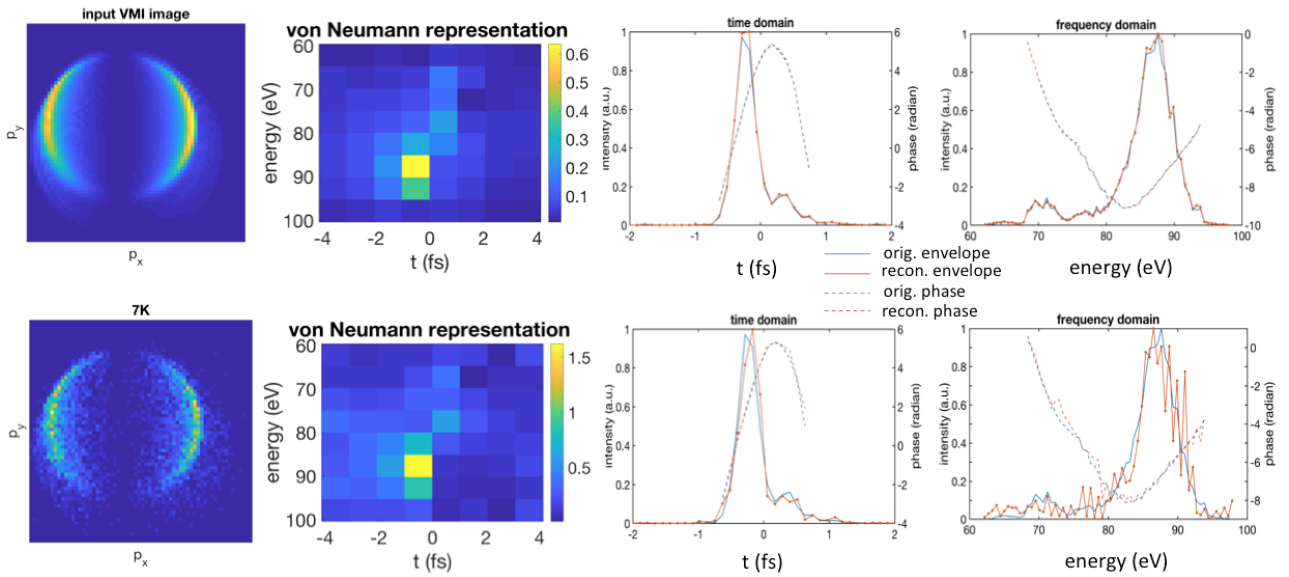

Figure 3: Example reconstruction of an attosecond x-ray pulse from genesis simulation. Top row from left to right: input 2-D momentum distribution; results of the nonlinear fitting algorithm to describe the x-ray pulse in the von Neumann representation; time domain reconstruction of the x-ray intensity; frequency domain reconstruction of the x-ray intensity. The bottom row is to show count statistics by sampling the simulated VMI image with Poisson noise of 7K particles.

time and frequency window, and i, j are indices that expand the frequency and time axes respectively (see details in [8]). We then obtain the basis functions $b_n(\vec{p})$ by plugging $\alpha_{\omega_i t_j}(t)$ into Eq. 1, and obtain B_{nm} using Eq. 3. Note that the index for the basis function n and m each spans the entire parameter space in time and frequency. In other words, $n = ij$, and it is the same for m. The von Neumann coefficients $Q_{i,j}$ are obtained by rearranging the 1-D coefficients c_n into a 2-D representation, where one axis is for time and the other is for frequency. The reconstructed x-ray electric field is $\vec{E}_{\text{recon}} = \sum_{i,j} Q_{i,j} \alpha_{\omega_i t_j}$.

Therefore the reconstruction problem is reduced to solving for the complex coefficients c_n. We define the cost function to be

$$cost = \sum_{p_x, p_y} \left| M(p_x, p_y) - B(p_x, p_y) \right|^2, \qquad (6)$$

where $M(p_x, p_y)$ is the measured photoelectron 2-D momentum distribution. We use Matlab's fminunc function to search for the complex coefficients c_n by minimizing the cost function. Figure 3 illustrates an example of the reconstruction result. We obtain the input pulse from a GENESIS simulation which has intricate substructures in the time and frequency domain. The algorithm successfully and completely reconstructs these structures. With count statistics of 7K particles sampled via Poisson noise, the algorithm is robust enough to still reconstruct the x-ray pulse in time and frequency domain.

It is worth noting the intricate structures in the GENESIS pulse which shows up as a second peak in time domain as well as frequency domain. The effect of the second bump in the x-ray pulse on the VMI detector image is an interference pattern of the photoelectron wave packet, which then is reflected in the interference fringes in the 2-D momentum distribution [13] (see the lower left corner of the VMI image in Fig. 3 for an example). Our reconstruction algorithm is capable of decoding such complicated quantum mechanical effects thanks to the complex coefficients that contain the phase information of the pulse. Further discussions on the algorithm's convergence, robustness, and limitations will be found in a future publication.

CONCLUSIONS

In this paper we discussed the working mechanism of angular streaking as diagnostic for attosecond x-ray pulses. We presented the novel co-linear VMI design with 3% energy resolution to measure photoelectron momentum distribution in the presence of a circularly polarized streaking laser. We showed the simulation results of the streaking process based on the Lewenstein model. Moreover, we described the nonlinear fitting algorithm that takes advantage of the von Neumann representation of any electric field. We demonstrated successful reconstruction of an attosecond x-ray pulse in both time and frequency domain. The outlook of this work is to utilize the angular streaking technique with experimentally produced attosecond x-ray pulses generated at LCLS.

ACKNOWLEDGEMENTS

This work was supported by the US Department of Energy, Office of Science, Basic Energy Sciences, Chemical Sciences, Geosciences, and Biosciences Division, under contract number DE-AC02-76SF00515 and DOE-BES Field Work Proposal 100317.

Content from this work may be used under the terms of the CC BY 3.0 licence (© 2018). Any distribution of this work must maintain attribution to the author(s), title of the work, publisher, and DOI.

ISBN: 978-3-95450-179-3 doi:10.18429/JACoW-FEL2017-WEP060

Content from this work may be used under the terms of the CC BY 3.0 licence (© 2018). Any distribution of this work must maintain attribution to the author(s), title of the work, publisher, and DOI.

REFERENCES

[1] P. B. Corkum, and F. Krausz, "Attosecond science," *Nature Physics* 3.6 (2007): 381.

[2] P. M. Paul *et al.*, "Observation of a train of attosecond pulses from high harmonic generation," *Science* 292.5522 (2001): 1689-1692.

[3] A. Zholents, "Method of an enhanced self-amplified spontaneous emission for x-ray free electron lasers." *Physical Review Special Topics-Accelerators and Beams* 8.4 (2005): 040701.

[4] J. MacArthur *et al.*, "High power sub-femtosecond X-ray pulse study for the LCLS." Proceedings of 8th Int. Particle Accelerator Conf.(IPAC'17), Copenhagen, Denmark, 14 - 19 May, 2017. (JACOW, Geneva, Switzerland, 2017.)

[5] J. Itatani *et al.*, "Attosecond streak camera," *Physical Review Letters* 88.17 (2002): 173903.

[6] P. Eckle *et al.*, "Attosecond angular streaking," *Nature Physics* 4.7 (2008): 565-570.

[7] N. Hartmann, G. Hartmann, and W. Helml, "Angle-resolved streaking for complete attosecond FEL pulse characterization," manuscript in preparation.

[8] S. Fechner *et al.*, "The von Neumann picture: a new representation for ultrashort laser pulses," *Optics Express*15.23 (2007): 15387-15401.

[9] N. G. Kling *et al.*, "Thick-lens velocity-map imaging spectrometer with high resolution for high-energy charged particles," *Journal of Instrumentation* 9.05 (2014): P05005.

[10] A. T. J. B. Eppink and D. H. Parker, "Velocity map imaging of ions and electrons using electrostatic lenses: Application in photoelectron and photofragment ion imaging of molecular oxygen," *Review of Scientific Instruments* 68.9 (1997): 3477-3484.

[11] M. Lewenstein *et al.*, "Theory of high-harmonic generation by low-frequency laser fields," *Physical Review A* 49.3 (1994): 2117.

[12] C. J. Dasch, "One-dimensional tomograttosecondaphy: a comparison of Abel, onion-peeling, and filtered backprojection methods," *Applied Optics* 31.8 (1992): 1146-1152.

[13] A. K. Kazansky *et al.*, "Interference effects in angular streaking with a rotating terahertz field," *Physical Review A* 93.1 (2016): 013407.